R E V I E W

Sabine Schmidt
Georg Eich
Sylviane Hanquinet
Heinz Tschäppeler
Peter Waibel
François Gudinchet

Extra-osseous involvement of Langerhans' cell histiocytosis in children

S. Schmidt (✉) · F. Gudinchet
Departments of Radiology and
Interventional Radiology,
University Hospital Centre—CHUV,
Lausanne, Switzerland
E-mail: sabine.schmidt@chuv.hospvd.ch
Tel.: +41-21-3144435

G. Eich
Department of Paediatric Radiology,
Children's Hospital, Zürich, Switzerland

S. Hanquinet
Department of Paediatric Radiology,
Hôpital Cantonal, Geneva, Switzerland

H. Tschäppeler
Department of Paediatric Radiology,
Children's Hospital, Bern, Switzerland

P. Waibel
Department of Paediatric Radiology,
Children's Hospital,
St. Gallen, Switzerland

Abstract The predominant clinical and radiological features of Langerhans' cell histiocytosis (LCH) in children are due to osseous involvement. Extra-osseous disease is far less common, occurring in association with bone disease or in isolation; nearly all anatomical sites may be affected and in very various combinations. The following article is based on a multicentre review of 31 children with extra-osseous LCH. The objective is to summarise the diverse possibilities of organ involvement. The radiological manifestations using different imaging modalities are rarely pathognomonic on their own. Nevertheless, familiarity with the imaging findings, especially in children with systemic disease, may be essential for early diagnosis.

Introduction

Langerhans' cell histiocytosis (LCH) is a rare disease of still unknown aetiology despite extensive research undertaken during recent decades. At present there are some hypotheses in favour of a primarily reactive, immunologically mediated origin, rather than a neoplastic process, but without any direct evidence of a viral stimulus or strong genetic component [1, 2].

In a multicentre study we reviewed the clinical data and radiological findings of 31 children being investi-gated and treated for extra-osseous biopsy-proven LCH between 1964 and 1999. There were 15 girls and 16 boys; the male:female ratio was 1:1.1. Age at diagnosis ranged from 3 months to 15 years (mean 2.8 years); 71% ($n=22$) were 3 years old or less. All patients routinely underwent radiographic skeletal survey, chest radiography and abdominal US. CT and MRI were performed according to the individual clinical indication, limited to the areas of histiocytic infiltration.

In all children, extra-osseous LCH had been histologically proven. Furthermore, the involvement of each

individual organ was inferred from biopsy and/or radiological findings.

Overview

Langerhans' cells are histiocytes of the dendritic cell lineage; they are defined as a cell type that had been recognised as a component of normal skin in the middle of the nineteeth century [3, 4, 5]. Histopathologically, LCH is characterised by a monoclonal proliferation of abnormal Langerhans' cells. This proliferation is thought to reflect an immune response to an as yet unknown antigenic stimulant [6]. These Langerhans' cells are capable of infiltrating almost any tissue or organ. The gold standard for diagnosis is electron microscopic study of the biopsy in which intracytoplasmic Birbeck granules of the Langerhans' cells are found; this is the only specific property of this phenotype [2, 7]. Secondarily, immunohistochemistry procedures are able to detect CD1 surface antigen on lesional cells, a less specific marker, having also been described in other histiocytic disorders such as rare cases of juvenile xanthogranuloma and Rosai-Dorfman disease (RDD) [2, 5]. The CD1a-positive cells can also found in bronchoalveolar lavage with a score higher than 5% [8, 9]. Finally, the positive stain of protein S-100 is commonly used in the evaluation of histiocytic disorders, although this is not a diagnostic marker on its own [2].

With an annual incidence of 2–5/1,000,000 of the paediatric population and a peak between 1 and 4 years of age, LCH is considered to be a mainly childhood disorder [1, 10]. The isolated pulmonary LCH seen in adults is considered a separate entity since it is strongly related to smoking, is polyclonal and frequently regresses [2, 11, 12].

LCH in children shows a heterogeneous clinical spectrum ranging from a single bone lesion to widespread multisystem disease. The clinical course is also very variable, mainly related to the patient's age and degree of organ dysfunction at the time of initial diagnosis. There has not yet been a generally accepted prognostic factor or a completely satisfactory clinical classification [13, 14]. Fatal outcome is seen in disseminated LCH, often affecting very young children (<2 years), and warrants aggressive therapy [1, 2, 10, 12, 15].

Plain radiography is the cornerstone of imaging of LCH, since bone lesions predominate in the majority of children. Osseous involvement has been described in the literature in great detail [10, 16]. The various imaging features of extra-osseous LCH, however, have been reported less often. They are often limited to isolated case reports [17, 18, 19, 20], or to single-organ involvement [21, 22, 23, 24, 25]. The objective of our descriptive analysis is to summarise the diverse radiological manifestations of the disease and to give an overview of the different imaging modalities now available to delineate disease extension.

Study population

We categorised the 31 children in our study into two groups: uni- or multifocal extra-osseous LCH. The frequency of involvement of the different organs, including proof by biopsy, can be seen in Table 1. Eleven children (35.5%) demonstrated unifocal extra-osseous LCH, five (16%) patients presented with disease in two organs, 11 (35.5%) with three, and four (14%) with four different organs infiltrated by LCH. Twenty-three (75%) of the 31 children showed extra-osseous and skeletal lesions simultaneously, of whom 19 (61%) had multifocal bone disease.

Thirty of 31 patients received systemic chemotherapy, two receiving additional radiation therapy for soft-tissue infiltration. One child had medical treatment only for diabetes insipidus.

Appropriate follow-up was available in 26 (84%) children; 19 (73%) demonstrated regression of clinical symptoms confirmed by radiological improvement without any major sequelae. Stable disease with significant organ dysfunction persisted in 5 (19%). Two children (8%) died from active disease.

Table 1 Frequency of organ involvement by extra-osseous LCH in 31 children, including proof by biopsy (*CSF* cerebral spinal fluid, *LCH* Langerhans' cell histiocytosis)

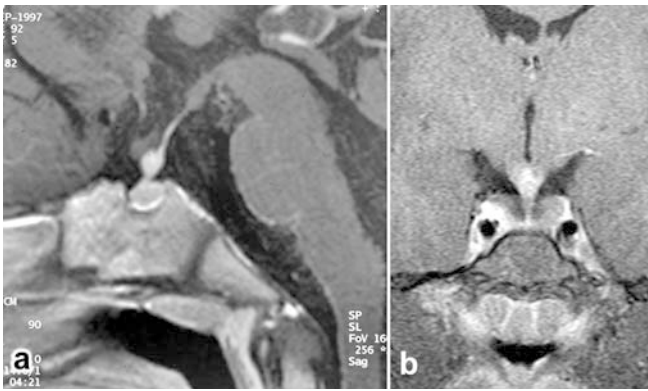| Organ	No of children ($n = 31$)	Unifocal extra-osseous LCH	Multifocal extra-osseous LCH	Individual proof by biopsy
Skin	17 (55%)	2	15	17
Brain	11 (35%)	4	7	3 (CSF)
Liver/biliary system/spleen	10 (32%)		10	7
Lung	8 (26%)	2	6	2
Soft-tissue mass	8 (26%)	1	7	6
Lymphadenopathy	8 (26%)	2	6	6
Bone marrow	6 (19%)		6	6
Parotid glands	2 (6%)		2	2
Gastrointestinal tract	2 (6%)		2	2

Fig. 1a, b Cerebral MRI in a 1-year-old boy with diabetes insipidus owing to LCH shows nodular thickening and enhancement of the pituitary stalk on sagittal (**a**) and coronal (**b**) T1-W spin-echo sequences after IV gadolinium

Radiological findings

Central nervous system

Cerebral LCH was seen in 11 (35%) of our 31 children, always following clinical symptoms of diabetes insipidus and radiologically characterised by infiltration of the pituitary gland (Fig. 1). In three children we also observed contrast-enhancing nodules in the temporal lobes, pons or cerebellum on MRI. One child showed orbital and paranasal sinus infiltration (Fig. 2) associated with osseous destruction. Chronic pituitary gland insufficiency occurred in all nine children with adequate follow-up, although the radiological findings regressed.

MRI is currently the modality of choice to detect cerebral LCH as well as involvement of the facial and extracranial soft tissues; the latter is often associated with adjacent osseous destruction. Pathologically, proliferation of the adventitial cells of blood vessels initially creates perivascular foci of Langerhans' cells. They later coalesce to granulomatous masses [26], which can be identified radiologically as cerebral, meningeal or spinal cord lesions. Brain parenchymal lesions may simply show demyelination and gliosis [22]. Involvement of the CNS is seen in 25–35% of cases during the course of disease, most often occurring in multisystem LCH [22, 27]. Thirty-five percent of our patients were thus affected, the majority with disseminated disease. The most common cerebral site is the hypothalamic-neurohypophyseal region [18, 27, 28], confirmed by our study. Radiological findings have been proven to correlate with clinical symptoms of diabetes insipidus [27]. Typically, they lead to lack of the normal neurohypophyseal high signal seen on T1-weighted (T1-W) MRI, frequently in association with a thickened and gradually enhancing pituitary stalk without wash-out (Fig. 1) [27, 28]. However, dynamic MRI has not proven useful for the differential diagnosis between LCH and other lesions, such as infundibular germ cell tumours [28].

The second-most-common site of CNS involvement is the cerebellum [29]. On MRI, cerebral parenchymal infiltration is characterised by small nodules, isointense on T1-W, iso- or mildly hyperintense on T2-W images and mostly enhancing after IV gadolinium [18, 22]. Very rarely, nodular meningeal thickening, spinal cord [30] or nerve root infiltration can be seen [31], and there is one biopsy-proven case report of histiocytic granuloma of the choroid plexus [32].

Salivary glands

Histiocytic infiltration of parotid glands was histologically proven in two of our patients and was detectable as bilateral symmetrical hyperplasia on US (Fig. 3a) and CT (Fig. 3b). In one case there was also involvement of submandibular glands. LCH of the parotid gland is extremely rare. We are unaware of any previous publication concerning children; there has been only one report of an adult heavy smoker [24]. Lieberman et al. [33] described involvement of parotid-associated lymphoid tissue. In our cases, chemotherapy was successful, the size of the parotid glands returning to normal (Fig. 3c) and there being no recurrence.

Fig. 2a, b A 3-year-old boy with systemic extra-osseous LCH. **a** Coronal and **b** sagittal T1-W spin-echo MRI after IV gadolinium demonstrate diffuse histiocytic infiltration of both orbital cavities extending into the paranasal sinuses and nasopharynx with osseous destruction
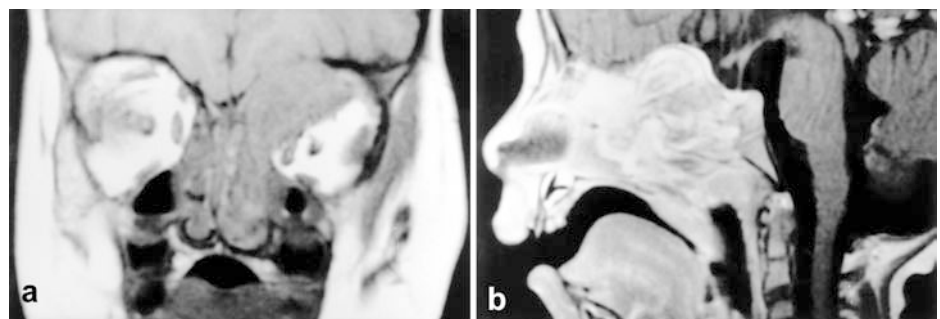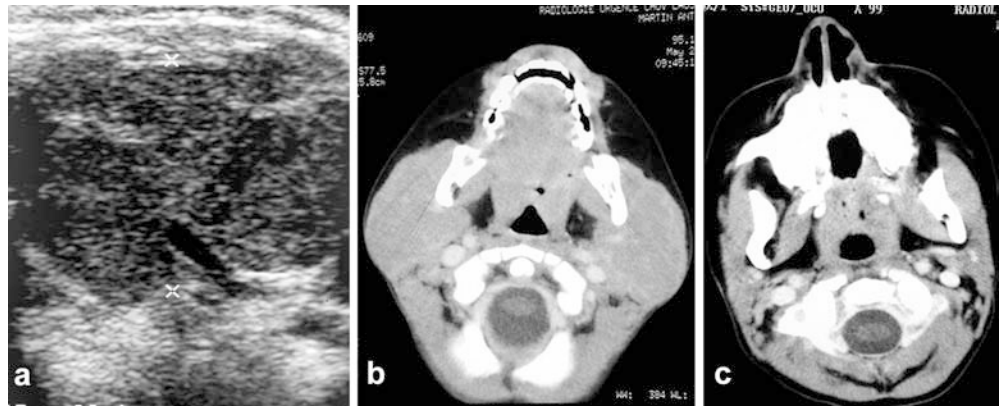
Fig. 3 a Cervical US of a 3-year-old boy demonstrates bilateral symmetrical enlargement of the parotid glands, confirmed by CT (**b**) and owing to diffuse histiocytic infiltration. **c** After chemotherapy size returned to normal 20 months later

Thymus

There was no patient in our study with biopsy-proven histiocytic infiltration of the thymus or alteration on imaging modalities. Radiological findings have been reported infrequently in small series, but unfortunately they have lacked histological proof [17, 21, 34]. It is always associated with multisystem LCH [21], usually pulmonary involvement [34]. Thymus gland involvement is probably more common than previously recognised [35]. Radiologically, it is characterized by diffuse enlargement with smooth or lobulated contour. CT may demonstrate cystic spaces corresponding to focal destructive lesions and serpentine calcifications of vascular or dystrophic origin [21, 34]. In general, treatment leads to complete regression, including the calcified and cystic areas. The main differential diagnosis is thymic rebound hyperplasia, i.e. transient thymic enlargement in a patient completing chemotherapy and resolving without further treatment.

Lungs

Pulmonary involvement occurs in 23–50% of children with LCH, similar to our study ($n=8$, 26%), and always as part of multisystem disease [24, 36, 37], also confirmed by our evaluation. When radiological findings and clinical symptoms are moderate and underlying LCH has already been recognised, proof by biopsy or bronchoalveolar lavage is not deemed necessary [23, 36].

In our eight patients, chest radiography demonstrated a uniform reticulonodular interstitial pattern. Two patients showed focal disease which regressed with chemotherapy. In the other six cases the radiological findings were diffuse; four evolved to chronic lung abnormalities and one of these died. Evolution in one 2-year-old boy was so aggressive that he required emergency treatment for acute hypoxia within 1 month of the diagnosis being established. Chest CT (Fig. 4a, b) revealed diffuse pulmonary emphysema and fibrosis complicated by pneumothorax, pneumomediastinum and subcutaneous emphysema extending as far as the scrotum.

Pathologically, histiocytic proliferation in the wall of the bronchioles and alveolar ducts causes destructive granulomas [38]. They are seen as pulmonary interstitial disease evolving from a reticulonodular to a honeycomb pattern on conventional chest radiography. Cavitation of these nodules leads to air trapping and airway obstruction, resulting in pulmonary cysts. Rarely, rupture of peripherally situated cysts results in spontaneous pneumothorax, which can become a life-threatening problem [36]. However, the very extensive bullous lesions we illustrate in Fig. 4 occur very infrequently. Pneumomediastinum might be associated, as was seen in our case, while pleural effusions and hilar or mediastinal lymphadenopathy is not common [38, 39], confirmed by our series of patients. Diffuse emphysema associated with pulmonary fibrosis is the end stage of this mixed restrictive and obstructive pattern [5, 23, 25, 36, 40, 41] (Fig. 4c–f).

High-resolution CT (HRCT) is the superior imaging modality for delineating nodules and cysts as well as the extent of disease [42]. It represents an excellent non-invasive means for diagnosis and follow-up of pulmonary LCH [43]. At the same time, HRCT is a substitute for monitoring the evolution in very young children too small for reliable respiratory function testing (RFT). Children are initially often asymptomatic; therefore, clinical findings are not helpful in the early detection of lung involvement by LCH [23, 36]. Conventional chest radiography might not show subtle findings when RFT are already abnormal [36], since histiocytic pulmonary infiltration gradually progresses [9]. HRCT can then be diagnostic. Typical findings of LCH, such as micronodules and/or thin-walled small cysts with irregular contour are easily detected [36, 42, 44]. They are bilateral and symmetrical, the cysts show slight upper-lobe predominance with relative sparing of the costophrenic angles. The main differential diagnoses of the HRCT findings are lymphangioleiomyomatosis, emphysema and cystic bronchiectasis.
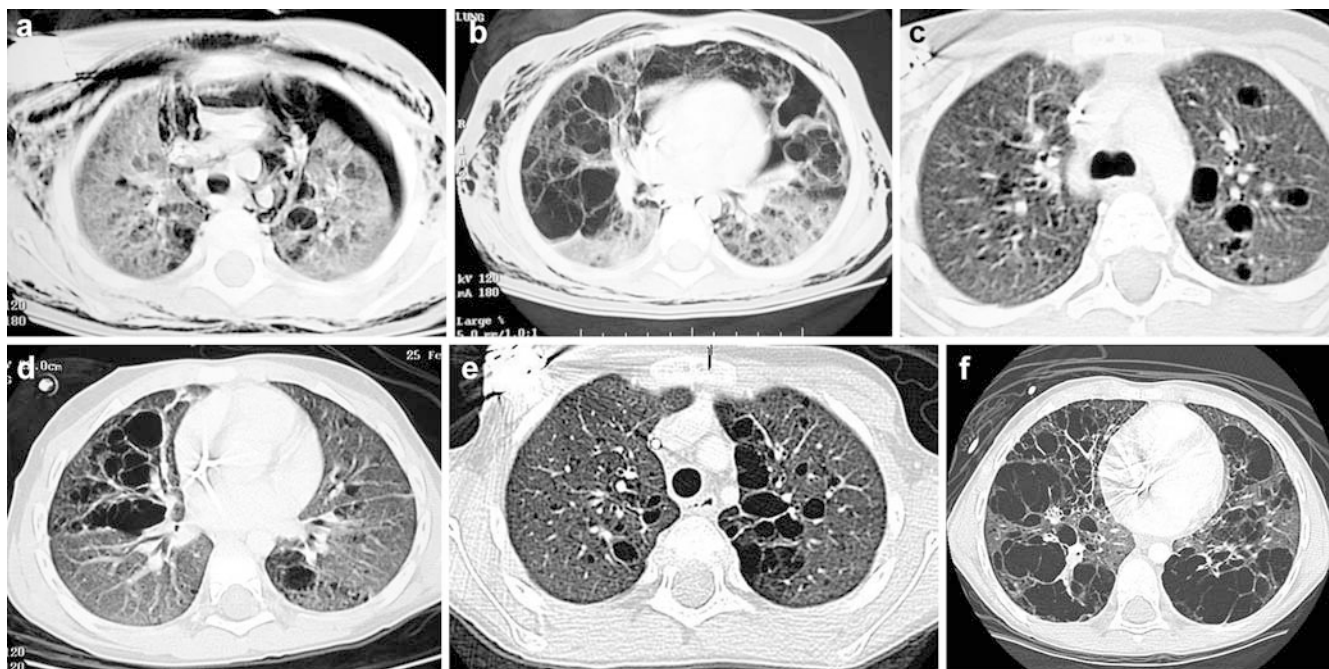
Fig. 4a–f Lung involvement by LCH in the same 3-year-old boy as in Fig. 3. **a, b** Chest CT performed as an emergency depicts multiple air-filled cysts and reticulonodular changes associated with acute spontaneous left anterolateral pneumothorax, pneumomediastinum and subcutaneous emphysema. **c, d** HRCT 20 months later. There is persisting lung emphysema with fibrosis characterising the chronic destruction of pulmonary parenchyma with regression of the acute involvement. **e, f** Follow-up by chest CT after a further 40 months shows slow, but irreversible progression of the lung emphysema without any acute complications

The diffuse interstitial and reticulonodular pattern seen on conventional chest radiography results from a summation of nodules and thin cystic walls [44]. According to Smets et al. [23] and Ha et al. [36], lung involvement by LCH does not adversely affect outcome, provided that treatment is adequate. Nevertheless, Bernstrand et al. [37] stressed that abnormal radiological findings, such as cysts, emphysema and/or fibrosis, persisted in 24% of patients with initial pulmonary LCH at long-term follow-up; however, the majority are or were smokers [37]. Possible toxicity of treatment on lungs might also lead to important sequelae and needs to be taken into consideration [23]. In our study, four of eight children with pulmonary involvement showed persistent lung abnormalities; one demonstrated slowly progressive lung emphysema after 5 years of follow-up (Fig. 4e, f).

Hepatobiliary system, spleen and gastrointestinal tract

Fifty to sixty percent of children with LCH demonstrate liver involvement, defined as hepatomegaly with or without liver dysfunction [45]. This is mostly a feature of multisystem disease, as confirmed by our study. The majority of our patients also had splenomegaly.

Hepatobiliary involvement by LCH was seen in 10 (32%) out of our 31 patients, the initial radiological findings being hepatosplenomegaly detected on abdominal US. In 4 children there was only moderate and homogeneous organ enlargement, returning to normal size after chemotherapy. In the other 6 patients we observed heterogeneous liver parenchyma on US and CT, with nodular and periportal hypoechogenicities or hypodensities corresponding to focal histiocytic inflammation (Fig. 5a). Biopsy revealed septal fibrosis and even biliary cirrhosis in 3 children with irregular segmental stenosis of bile ducts alternating with areas of dilatation. In 2, retrograde cholangiography demonstrated features of sclerosing cholangitis (Fig. 6). One of the three children with cirrhosis died, another underwent successful liver transplantation, while the third could not be followed up since parents refused liver transplantation. Hepatosplenomegaly as well as focal liver lesions in the other patients gradually regressed with chemotherapy (Fig. 5b). However, follow-up CT at 5 years demonstrated recurrence of liver hypodensities in one patient (Fig. 5c).

Histologically, hepatic involvement by LCH is characterised by periportal histiocytic infiltration evolving in four phases: from an initial proliferative phase to a granulomatous, xanthomatous and finally to a fibrous phase [46, 47]. Hepatomegaly and the different stages can be well depicted on US, CT and MRI [5, 45, 48, 49, 50]. Periportal hypoechoic changes correspond to hypodensities on CT and to moderate-to-high intensities on T2-W MRI, reflecting the proliferative and granuloma-

318

Fig. 5 a Abdominal CT on the same 3-year-old boy as in Fig. 4 depicts hepatosplenomegaly with multiple small hypodense nodules disseminated throughout the liver parenchyma reflecting histiocytic periportal infiltration. **b** Twelve months later, follow-up CT demonstrates subtotal regression of the periportal infiltration with persisting moderate hepatosplenomegaly and two focal hypodensities in the left lobe of the liver. **c** However, CT 50 months later demonstrates confluent geographical hypodensities in the liver parenchyma, this time without circumscribed nodules

tous phases. They result from infiltration by histiocytes and other inflammatory cells surrounded by oedema. Periportal contrast enhancement is then seen, suggesting portal triaditis. Subsequent change to hyperechoic nodules, which are composed of fat, occurs as a result of evolution into the xanthomatous phase. They remain hypodense on CT, while on MRI this stage is characterised by hyperintensities on T1-W images, being hypointense on T2-W images [49, 50, 51]. Finally, micronodular biliary cirrhosis results from extensive periductal and periductular fibrosis associated with sclerosing cholangitis [45, 46]. The segmental biliary stenoses and asymmetrical dilatations can be detected by conventional cholangiography (Fig. 6), or magnetic resonance cholangiopancreatography (MRCP). At this
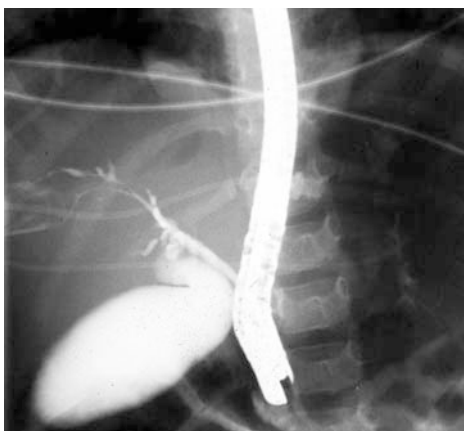

Fig. 6 Biliary cirrhosis and sclerosing cholangitis due to LCH in a 3-year-old girl. Retrograde cholangiography demonstrates lack of opacification of the left intrahepatic bile ducts, while an arc-like deviation and intraluminal irregularities are seen in the biliary system of the right lobe

stage, liver transplantation is the treatment of choice [45], which was performed in one of our patients.

LCH involvement of the gastrointestinal tract is very rarely seen, as was the case in our study ($n=2$, 6%, Table 1). It occurs in about 2% of systemic LCH in large series [48, 52] and little is known about its clinical course. However, it might be underdiagnosed because digestive symptoms are very non-specific and are often attributed to other aspects of the illness, such as side effects of the treatment [52]. According to Geissmann et al. [48], it is always associated with multisystem disease and considered as one clinicopathological entity, together with mucosal and cutaneous LCH, a feature confirmed by our two cases and by other published case reports [15, 20, 53]. Thus children with cutaneous LCH and digestive symptoms, such as malabsorption, diarrhoea or failure to thrive, should undergo gastrointestinal tract biopsies [48].

The two cases with gastrointestinal involvement in our study were proven by biopsy. One demonstrated disease limited to the distal colon, while the other showed histiocytic infiltration of the duodenal wall. MRI detected nodular parietal thickening of the rectosigmoid in the first case. Diagnostic procedures for the second child were limited to gastroscopy and colonoscopy with proof by biopsy. Unfortunately, neither could be followed up long term.

Histopathologically, gastrointestinal LCH is characterised by histiocytic infiltration of the lamina propria and submucosa with consecutive irregular mucosal thickening and erosions, followed by mucosal and glandular atrophy [54]. On small bowel enema features, LCH involvement is characterised by loss of the typical mucosal pattern, appearance of the cobblestone feature, segmental luminal narrowing and separation of loops [5, 15, 48]. These radiological findings are generally indistinguishable from those of other exudative enteropathies and inflammatory bowel diseases. Enlarged mesenteric or other lymph nodes are not a particular association [20, 48]. In our study, two children demonstrated biopsy-proven histiocytic infiltration of the rectum and sigmoid colon, one of whom had nodular infiltration of distal colonic wall visible on CT. To our knowledge there has not been any publication of the
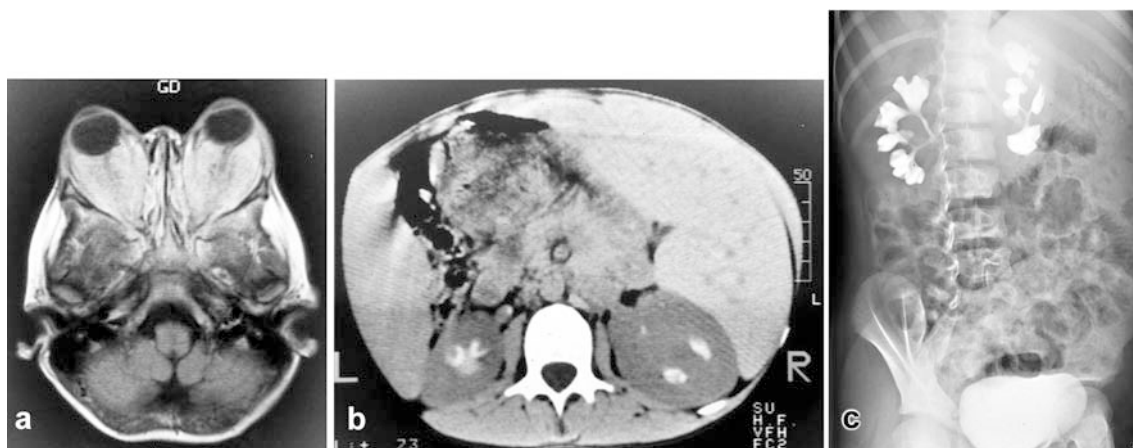
Fig. 7a–c A 4-year-old boy with extranodal multisystem Rosai Dorfman disease. **a** Contrast-enhanced brain CT shows bilateral expansive intraconal infiltration of retro-orbital fat by histiocytes. The adjacent osseous structures, globes and optic nerves are spared; the latter are surrounded by the inflammatory process. **b** Abdominal CT demonstrates massive proliferation of histiocytes within the hilus and pelvis of both kidneys with compression of calyces and ureters. These features are also seen on intravenous urography (**c**). There was concomitant invasion of the lumbar and sacral spinal canal, including the anterior epidural space and both foramina on MRI (not shown)

radiological findings of colonic involvement by LCH, nor has there been any publication of the CT or MRI features of histiocytic infiltration of small or large bowel. However, they are very non-specific, similar to any colitis of inflammatory, infectious or ischaemic origin. Outcome is clearly related to extension of disease and age of the child; intestinal dysfunction may persist for a long time after treatment [48]. Clinical improvement goes along with gradual reappearance of the mucosal pattern on conventional bowel studies, which might still be coarse [20].

Skin

Cutaneous LCH is very common, seen in 50% of all cases [55] and confirmed by our review. It is not necessarily considered as a benign feature, as many patients progress to disseminated disease, which is also true for our study. Fifteen of 17 children with skin involvement had multifocal extra-osseous LCH.

Rosai-Dorfman disease

In addition to the 31 children showing extra-osseous LCH, our retrospective study revealed one 4-year-old boy (Fig. 7) with another histiocytic syndrome which occurs predominantly in children. RDD, or sinus histiocytosis with massive lymphadenopathy, is a transitional form between LCH and non-LCH pathologies. It is an uncommon proliferative disorder of histiocytes, first described in 1969 [56]. Like LCH, the aetiology is still unknown. It is generally thought to be a benign process, a disorder of immune regulation or response to a presumed infectious agent. Major manifestations are seen in the lymph nodes with resulting proliferation of sinusoidal histiocytes [57]. The characteristic histological feature is distension of sinusoids by histiocytes containing one or more intact lymphocytes. Both Langerhans' cells and the histiocytes of RDD are S-110 protein positive, but the latter do not contain Birbeck granules. The presence of lymphophagocytic histiocytes and S-100 protein positivity is regarded as diagnostic of RDD [56, 57].

The most frequent clinical manifestation of RDD is bilateral, non-tender, painless cervical lymphadenopathy up to 6 cm in diameter. Extranodal multisystem disease is rare and can be difficult to differentiate from LCH [58, 59]. Our child showed orbital involvement expressed as bilateral exophthalmos (Fig. 7a). Histologically, there was diffuse histiocytic infiltration of retro-orbital fat. Two treatments with corticosteroids led to temporary regression, followed by local recurrence, which on the second occasion was associated with hepatosplenomegaly and retroperitoneal involvement (Fig. 7b). Bilateral renal pelvic inflammatory masses resulting in extrinsic ureteric and calyceal compression (Fig. 7c) extended to the lumbar and sacral spine; there was infiltration of the anterior epidural space and spinal foramina on both sides from L1 to S2.

In general, RDD is considered as pseudotumoural benign disease with self-limiting course. However, aggressive behaviour has been reported, as in our child who finally underwent surgery. The mortality is 7%, mostly from complications and especially of the renal system [57].

Conclusions

There are very few publications concerning the various radiological findings of all organs involved by LCH in children, and the focus has been on osseous involvement [25]. Extra-osseous LCH is characterised by many different possibilities for organ involvement, resulting in a great variety of clinical manifestations and radiological findings, none being pathognomonic in isolation. The severity and pattern of the abnormality at the onset of the disease, as well as monitoring of regression of tissue infiltration, can be precisely monitored by the specific imaging modalities currently available, e.g. MRI for cerebral, osteoarticular and soft-tissue disease. MRCP non-invasively detects infiltration of bile ducts and additional sequences simultaneously evaluate hepatic parenchyma. Spiral CT is still best indicated for pulmonary and mediastinal lesions. HRCT may be a substitute for RFT in assessing and monitoring the extension of pulmonary involvement in LCH, especially in very young children who are too small for reliable RFT.

References

1. Nicholson HS, Egeler PM, Nexbit ME (1998) The epidemiology of Langerhans' cell histiocytosis. Hematol Oncol Clin North Am 12:379–383
2. Favara BE, Feller AC, Pauli M, et al (1997) Contemporary classification of histiocytic disorders. Med Pediatr Oncol 29:157–166
3. Langerhans P (1868) Ueber die Nerven der menschlichen Haut. Virchows Arch (Pathol Anat) 44:325–337
4. Devay KO, Putzi MJ (1997) Clinico-pathological consultation—head and neck Langerhans' cell histiocytosis. Ann Otol Rhinol Laryngol 106:526–532
5. Egeler RM, D'Angio GJ (1995) Langerhans' cell histiocytosis. J Pediatr 127:1–10
6. Nezelof C, Basset F (1998) Langerhans' cell histiocytosis research. Hematol Oncol Clin North Am 12:385–406
7. Birbeck W, Breathnach AS, Everall JD (1961) An electron microscopic study of basal melanocytes and high-level clear cells (Langerhans' cells) in vitiligo. J Invest Dermatol 37:51–60
8. Auerswald U, Barth J, Magnussen H (1991) Value of CD-1-positive cells in bronchoalveolar lavage fluid for the diagnosis of pulmonary histiocytosis X. Lungs 169:305–309
9. Réfabert L, Rambaud C, Mamou-Mani T, et al (1996) Cd1a-positive cells in bronchoalveolar lavage samples from children with Langerhans' cell histiocytosis. J Pediatr 129:913–915
10. Kilpatrick SE, Wenger DE, Gilchrist GS, et al (1995) Langerhans' cell histiocytosis of bone. Cancer 76:2471–2484
11. Yousem SA, Colby TV, Chen YY, et al (2001) Pulmonary Langerhans' cell histiocytosis: molecular analysis of clonality. Am J Surg Pathol 25:630–636
12. Howarth DM, Glichrist GS, Mullan BP, et al (1999) Langerhans' cell histiocytosis. Diagnosis, natural history, management, and outcome. Cancer 85:2278–2290
13. Broadbent V, Egeler RM, Nesbit ME Jr (1994) Langerhans' Cell histiocytosis: clinical and epidemiological aspects. Br J Cancer 70[Suppl XXIII]:S11–S16
14. Chu T, D'Angio GJ, Favara B, et al (1987) Histiocytosis syndromes in children: by the writing group of the Histiocyte Society. Lancet 1:208–209
15. Damry N, Hottat N, Azzi N, et al (2000) Unusual findings in two cases of Langerhans' cell histiocytosis. Pediatr Radiol 30:196–199
16. Fernandez-Latorre F, Menor-Serrano F, Alonso-Charterina S, et al (2000) Langerhans' cell histiocytosis of the temporal bone in pediatric patients: imaging and follow-up. AJR Am J Roentgenol 174:217–221
17. Abramson SJ, Berdon WE, Reilly BJ, et al (1987) Cavitation of anterior mediastinal masses in children with histiocytosis-X. Report of four cases with radiographic, pathologic findings and clinical follow-up. Pediatr Radiol 17:10–14
18. Strottmann JM, Ginsberg LE, Stanton C (1995) Langerhans' cell histiocytosis involving the corpus callosum and cerebellum: gadolinium-enhanced MRI. Neuroradiology 37:289–292
19. Kim E-Y, Choi J-U, Kim T-S, et al (1995) Huge Langerhans' cell histiocytosis granuloma of choroid plexus in a child with Hand-Schüller-Christian disease. J Neurosurg 92:1080–1084
20. Patel BJ, Chippindale AJ, Gupta SC (1991) Case report: small bowel histiocytosis-X. Clin Radiol 44:62–63
21. Junewick JJ, Fitzgerald NE (1999) The thymus in Langerhans' cell histiocytosis. Pediatr Radiol 29:904–907
22. Poe LB, Dubowy RL, Hochhauser L, et al (1994) Demyelinating and gliotic cerebellar lesions in Langerhans' cell histiocytosis. AJNR Am J Neuroradiol 15:1919–1928
23. Smets A, Mortele K, De Praeter G, et al (1997) Pulmonary and mediastinal lesions in children with Langerhans' cell histiocytosis. Pediatr Radiol 27:873–876
24. Darvishian F, Hirawat S, Teichberg S, et al (2002) Langerhans' cell histiocytosis in the parotid gland. Ann Clin Sci 32:201–206
25. Meyer JS, Harty MP, Mahboubi S, et al (1995) Langerhans' cell histiocytosis: presentation and evolution of radiologic findings with clinical correlation. Radiographics 15:1135–1146
26. Kepes JJ, Kepes M (1969) Predominantly cerebral forms of histiocytosis X. A reappraisal of "Gagel's hypothalamic granuloma", "granuloma infiltrans of the hypothalamus" and "Ayala's disease" with a report of four cases. Acta Neuropathol 14:77–98
27. Maghnie M, Arico M, Vill A, et al (1992) MR of the hypothalamic-pituitary axis in Langerhans cell histiocytosis. Am J AJNR Neuroradiol 13:1365–1371
28. Liang I, Korogi Y, Sugahar T, et al (2000) Dynamic MR imaging of neurohypophyseal germ cell tumors for differential diagnosis infundibular diseases. Acta Radiol 41:562–566
29. Favara BE, Jaffe T (1987) Pathology of Langerhans' cell histiocytosis. Hematol Oncol Clin North Am 1:75–97
30. Hamilton B, Connolly ES, Mitchell WT (1995) Isolated intramedullary histiocytosis X of the cervical spinal cord. J Neurosurg 83:716–718
31. Lacroix M, Farmer JP, Meagher-Villemure K, et al (1996) Cauda equina histiocytosis X. Pediatr Neurol 14:231–235

32. Eung-Young K, Joong-Uhn C, Tai-Seung K, et al (1995) Huge Langerhans' cell histiocytosis granuloma of choroid plexus in a child with Hand-Schüller-Christian disease. J Neurosurg 83:1080–1084

33. Liebermann PH, Jones CR, Steinman RM, et al (1996) Langerhans' cell (eosinophilic) granulomatosis: a clinicopathologic study encompassing 50 years: Am J Surg Pathol 20:519–552

34. Sumner TE, Auringer ST, Preston AA (1993) Thymic calcifications in histiocytosis X. Pediatr Radiol 23:204–205

35. Newton WA, Hamoudi AB, Shannon BR (1987) Role of the thymus in histiocytosis-X. Hematol Oncol Clin North Am 1:63–74

36. Ha SY, Helms P, Fletcher M, et al (1992) Lung involvement in Langerhans' cell histiocytosis: prevalence, clinical features and outcome. Pediatrics 89:466–469

37. Bernstrand C, Cederlund K, Sandstedt B, et al (2001) Pulmonary abnormalities at long-term follow-up of patients with Langerhans' cell histiocytosis. Med Pediatr Oncol 36:459–468

38. Soler P, Tazi A, Hance AJ (1995) Pulmonary Langerhans' cell granulomatosis. Curr Opin Pulm Med 1:406–416

39. Shaker KG, Umall CB, Fraire AE (1995) Langerhans' cell histiocytosis of the lung in association with mediastinal lymphadenopathy. Pathol Int 45:762–766

40. Kulwiec EL, Lynch Da, Aguayo SM, et al (1992) Imaging of pulmonary histiocytosis X. Radiographics 12:515–526

41. Meyer JS, De Camargo B (1998) The role of radiology in the diagnosis and follow up of Langerhans' cell histiocytosis. Hematol Oncol Clin North Am 12:307–326

42. Brauner MW, Grenier P, Mouelhi MM, et al (1989) Pulmonary histiocytosis X: evaluation with high-resolution CT. Radiology 172:255–258

43. Koh DM, Hansell DM (2000) Computed tomography of diffuse interstitial lung disease in children. Clin Radiol 55:659–667

44. Moore AD, Godwin JD, Müller NL, et al (1989) Pulmonary histiocytosis X: comparison of radiographic and CT findings. Radiology 172:249–254

45. Braier J, Ciocca M, Latella A, et al (2002) Cholestasis, sclerosing cholangitis, and liver transplantation in Langerhans' cell histiocytosis. Med Pediatr Oncol 38:178–182

46. Sisto A, Feldman P, Garel L, et al (1987) Primary sclerosing cholangitis: study of five cases and review of literature. Pediatrics 80:918–923

47. Kaplan KJ, Goodman ZD, Ishak KG (1999) Liver involvement in Langerhans' cell histiocytosis: a study of nine cases. Mod Pathol 12:370–378

48. Geissmann F, Thoma C, Emile JF, et al (1996) Digestive tract involvement in Langerhans' cell histiocytosis. J Pediatr 129:836–845

49. Chan YL, Li CK, Lee CY (1997) Sonographic appearance of hepatic Langerhans' cell histiocytosis. Clin Radiol 52:761–763

50. Kim M, Lyu C, Jin Y, et al (1999) Langerhans' cell histiocytosis as a cause of periportal abnormal signal intensity on MRI. Abdom Imaging 24:373–377

51. Arakawa A, Matsukawa T, Yamashita X, et al (1994) Periportal fibrosis in Langerhans' cell histiocytosis mimicking multiple liver tumors: US, CT and MR findings. J Comput Assist Tomogr 18:157–159

52. Nanduri VR, Kara K, Malone M, et al (1999) Colon involvement in Langerhans' cell histiocytosis. J Pediatr Gastroenterol Nutr 29:462–466

53. Couderc L, Vannier JP, Marret S, et al (1997) Neonatal exudative enteropathy and Langerhans' cell histiocytosis (in French). Arch Pediatr 4:1155

54. Stuphen JL, Fechner RE (1986) Chronic gastroenteritis in a patient with histiocytosis X. J Pediatr Gastroenterol Nutr 5:324–328

55. Chu T, Jaffe R (1994) The normal Langerhans' cell and the CLH cell. Br J Cancer 70:4–10

56. Rosai J, Dorfman RF (1969) Sinus histiocytosis with massive lymphadenopathy. Arch Pathol 87:63–70

57. McAlister WH, Herman T, Dehner LP (1990) Sinus histiocytosis with massive lymphadenopathy (Rosai-Dorfman disease). Pediatr Radiol 20:425–432

58. Levine EA, Landry MM (1994) Rosai-Dorfman disease of soft tissue. Surgery 155:650–652

59. Kugler A, Middel P, Gross AJ, et al (1997) Unusual bilateral renal histiocytosis: extranodal variant of Rosai-Dorfman disease. Arch Pathol Lab Med 116:1366–1367